LiI-Doped *N,N*-Dimethyl-pyrrolidinium Iodide, an Archetypal Rotator-Phase Ionic Conductor

Josefina Adebahr,*,† Aaron J. Seeber,† Douglas R. MacFarlane,‡ and Maria Forsyth*,†

School of Physics and Materials Engineering and School of Chemistry, and the ARC Centre for Nanostructured Electromaterials, Monash University, Clayton 3800, Victoria, Australia

Received: April 14, 2005; In Final Form: August 24, 2005

N,N-Dimethyl-pyrrolidinium iodide, and the effect of doping with LiI, has been investigated using DSC, NMR, and impedance spectroscopy. It was found that the addition of a small amount of LiI enhances the ionic conductivity by up to 3 orders of magnitude for this ionic solid. Furthermore, a slight decrease in phase transition onset temperatures, as well as the appearance of a superimposed narrow line in the ^{1}H NMR spectra with dopant, suggest that the LiI facilitates the mobility of the matrix material, possibly by the introduction of vacancies within the lattice. ^{7}Li NMR line width measurements reveal a narrow Li line width, decreasing in width and increasing in intensity with temperature, indicating mobile Li ions.

Introduction

Solid materials, in which one component is able to move much faster than the others, are usually referred to as fast-ion conductors, which is a well-known phenomenon in materials such as ceramics and glasses.[1,2] Because of the high ionic mobility within these materials, conductivities of the same order of magnitude as molten salts, or aqueous solutions, can be achieved. Mixed ionic conductors, for example AgI and AgBr mixtures, have shown up to 3 orders of magnitude increase in conductivity compared to the pure systems. This has been attributed to a distortion of the lattice with the incorporation of ions of different size compared to the host matrix.[3]

Doped ionic plastic crystals (crystalline materials that can deform easily without fracture under an applied force) have shown a remarkable increase in conductivity, even at very low doping levels, indicating a fast-ion conduction mechanism.[4−7] For example, the addition of a small amount of a lithium salt to the plastic crystal ethyl methyl pyrrolidinium bis(trifluoromethanesulfonyl)amide, showed a more than 2 orders of magnitude increase in conductivity, giving values $\sim 10^{-2}-10^{-3}$ S/cm in the plastic phase, i.e., approaching values useful in applications such as lithium batteries.[4,8] The material investigated here, *N,N*-dimethyl-pyrrolidinium iodide, is one of the structurally simplest salts in the pyrrolidinium cation family. This family of salts include materials displaying both rotator as well as plastic crystal phases.[9−13] Plastic phases have been observed for salts with anions having delocalized charges, such as tetrafluoroborate and bis(trifluoromethanesulfonyl)amide (TFSA), as opposed to the simple iodide anion used here. However, an earlier investigation on the iodide salt has shown that this material exhibits rotator phases (i.e., phases in which there are rotational degrees of freedom).[14]

The transport mechanism for the lithium ions in this type of material is a focus of current research. One hypothesis is the "paddle-wheel mechanism", which has been shown to be the main factor in cation transport in inorganic plastic crystals such as Li_2SO_4 and Na_3PO_4.[15,16] Another hypothesis is an increased mobility of the ions in the grain boundaries due to a higher concentration of vacancies/dislocations.[13,17] The effect of grain boundaries in polycrystalline materials as well as mixed ion conductors such as $AgCl/Al_2O_3$, ZrO_2/O_2, etc. is a well-known phenomenon and has been discussed in terms of space charge distribution by Maier et al.[18]

The addition of LiI to the ionic solid *N,N*-dimethyl-pyrrolidinium iodide ($P_{1,1}I$) has been investigated here. The $P_{1,1}I$ matrix material has not shown any plastic properties, although it goes through 2 phase transitions before decomposing; these transitions have been linked previously to the onset of different rotational motions of the pyrrolidinium cation.[14] It is the simplest member of a family of a large range of plastic crystals based on the pyrrolidinium cation and, as such, is of interest as a model system for the investigation of this family of pyrrolidinium salts in general.

Experimental Section

Samples. Pure *N,N*-dimethyl-pyrrolidinium iodide, abbreviated $P_{1,1}I$, was prepared from 1-methyl-pyrrolidine and iodomethane, according to methods detailed elsewhere.[9] Doping with LiI was carried out via solvent casting in a drybox, whereby $P_{1,1}I$ and LiI were dissolved together in acetonitrile, at a ratio of 1 g of sample to 20 mL of acetonitrile. The acetonitrile was then evaporated under dry N_2, and finally, the doped samples were dried under vacuum at 70 °C for at least 48 h. Samples with 2, 5, and 10 wt % LiI in $P_{1,1}I$ were made.

Thermal Analysis. A Perkin-Elmer differential scanning calorimeter (DSC) model 7 was used to measure the thermal properties of the samples, over a temperature range of 323−503 K with a scanning rate of 10 K min^{-1}. The pure $P_{1,1}I$ decomposes before melting and is a stable solid up to ~520 K.

NMR Spectroscopy. ^{1}H NMR line width measurements were performed on a Bruker AS300 pulse NMR spectrometer operating at a Larmor frequency of 300.14 MHz, using a single $\pi/4$ pulse of 1.5 μs, a recycle delay of 6 s, and 32 scans. ^{7}Li NMR line width measurements were performed on the same spectrometer, operating at a Larmor frequency of 116 MHz,

* Corresponding authors. E-mail: josefina.adebahr@eng.monash.edu.au (J.A.); maria.forsyth@eng.monash.edu.au (M.F.). Telephone: 61 3 99054939. Fax: 61 3 99054940.

† School of Physics and Materials Engineering.

‡ School of Chemistry.

10.1021/jp051927u CCC: $30.25
Published on Web 10/07/2005

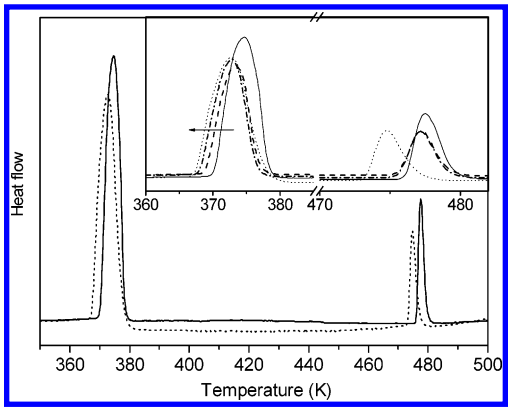

Figure 1. The DSC traces for pure $P_{1,1}I$ (solid line) and $P_{1,1}I$ doped with 10 wt % LiI (dotted line). Inset shows the two phase transitions at ~373 and ~478 K for the pure $P_{1,1}I$ (—) compared to samples with 2 (– – –), 5 (– · – · – ·) and 10 (···) wt % LiI. The arrow shows increasing doping content.

TABLE 1: Onset Temperature, Enthalpy, and Entropy Change (Based on Mol Matrix Material) for the Two Transitions for the 4 Different Samples

	III → II transition			II → I transition		
	T (K)	$\Delta_{tr}H$ (kJ/mol)	$\Delta_{tr}S$ (J/Kmol)	T (K)	$\Delta_{tr}H$ (kJ/mol)	$\Delta_{tr}S$ (J/Kmol)
$P_{1,1}I$	370.4	14.1	38.1	476.3	2.7	5.7
$P_{1,1}I$ 2 wt % LiI	369.1	13.6	36.9	474.8	2.5	5.3
$P_{1,1}I$ 5 wt % LiI	368.2	11.9	32.3	474.8	2.0	4.2
$P_{1,1}I$ 10 wt %LiI	366.5	10.6	28.9	473.5	1.6	3.4

using a single $\pi/4$ pulse of 3 μs, a recycle delay of 6 s, and 32 scans. At all temperatures, the probehead was allowed to equilibrate for 20 min before tuning and data collection. The deconvolution of the spectra was done by fitting the peaks with Gaussian or mixed Gaussian/Lorentzian functions, and the error of the fitting has been estimated to be less than 10%.

Conductivity. Conductivity measurements were carried out on a Solartron frequency response analyzer (FRA) model 1296, driven by Solartron impedance measurements software version 3.2.0 over a frequency range of 1 MHz to 0.01 Hz with a signal voltage of 0.1 V. The samples were pressed into pellets and thereafter sandwiched between two stainless steel blocking electrodes. Measurements were taken at 10 K intervals. The cell temperature was controlled using a Eurotherm control model 2204. The temperature was measured using a type K thermocouple with an accuracy of ±1°. The conductance of the samples was determined from the real axis intercept in the Nyquist plot of the impedance data.

Results and Discussion

The thermal behavior of the pure $P_{1,1}I$ sample and the $P_{1,1}I$ doped with 10 wt % lithium iodide is shown in the DSC traces presented in Figure 1. No transitions were recorded at low temperatures, and both samples show two exothermic solid−solid transitions, one around 373 K and one around 478 K. Both phase transitions are shifted toward lower temperatures when doping with LiI, as can be seen in the inset in Figure 1, where the two transitions are enlarged and shown as a function of temperature for the 4 different samples (pure $P_{1,1}I$ and $P_{1,1}I$ doped with 2, 5, and 10 wt % LiI). In Table 1, the onset temperatures of the transitions, as well as their enthalpy and entropy changes are summarized. It can be seen that the onset temperature decreases with increasing amount of LiI. It can also be noted from Table 1 that the enthalpy and entropy changes (calculated per mol $P_{1,1}I$ in each sample) of the phase transitions decrease as a function of doping content. The slight decrease in the entropy and enthalpy of the transition could be brought about by the appearance of defected/amorphous regions.

The fact that the addition of LiI to the matrix material causes a lowering of the transition temperatures, which can be linked to small changes in the enthalpy and entropy of the transitions, ΔH_{tr} and ΔS_{tr}, is strong evidence that the Li ions have been incorporated into the bulk matrix to form a solid solution. The transition temperature in each case is the point at which the chemical potentials of each component in the two phases equate, i.e., if μ_1 is the chemical potential of $P_{1,1}I$, then $\mu_1(I) = \mu_1(II)$ at the transition temperature, and because the solubility of LiI in phase II is likely to be less than in phase I, then the temperature at which $\mu_1(I) = \mu_1(II)$ will be lower for the higher LiI content. This will lead to a decrease in the transition temperature. It is also possible, however, for the differences in solubility of the second component in the two solid solution phases to be inverted, and in this case, the transition temperature would rise; while in the case where the solubility is comparable in the two phases, then the transition temperature will remain approximately constant. The range of phenomena is well exemplified by the effect of a second component on the $\alpha \rightarrow \beta$ solid−solid transition at 883 °C in metallic Ti;[19] addition of aluminum to Ti to form the binary alloy causes the transition to rise sharply, whereas addition of vanadium causes an equally sharp fall. A decrease in the phase transition temperature with increasing amount of dopant has also previously been observed in mixtures of inorganic molten salts, for example, $BaTiO_3$−$BaCl_2$.[20] The significance of the changes here is chiefly that they provide evidence for the existence of solid solubility in this binary system.

In previous work based on pyrrolidinium bis(trifluoromethane sulfonyl)amide salts displaying plastic crystal behavior, there has been some debate as to whether solid solutions of lithium salts in these matrixes can really exist or whether a mixture of pure compounds is more likely.[5,21] In that case, the solid−solid phase transition certainly did not change as dramatically as it does in the present iodide system, and so it is more difficult to make a conclusive argument. In this case, however, it would appear that the addition of LiI to the $P_{1,1}I$ matrix causes sufficient disruption to the matrix so as to change the solid−solid phase transition temperature. This presents, therefore, the first direct evidence of solid solution behavior in the pyrrolidinium family of salts.

$P_{1,1}I$ decomposes before melting, which means that Timmerman's criteria for the existence of plastic phases, that the final entropy of melting should be less than 20 J K^{-1} mol^{-1}, cannot be applied to this material. However, the material has not shown any visible plasticity, e.g., there is no deformation of the sample when taken up to 240 °C in the conductivity cell, which is well above the II → I transition. Therefore, it is believed that this material is not truly a plastic crystal even though it belongs to a family of salts that are highly plastic in nature; some examples are dimethyl pyrrolidinium tetrafluoroborate, dimethyl pyrrolidinium thiocyanate, etc. As has been discussed in an earlier publication, the pyrrolidinium cation in $P_{1,1}I$ exhibits rotational degrees of freedom in the higher temperature phases; however, for a material to have plastic properties, it is believed that both the cation and the anion of the matrix materials have to be mobile. Because of the lack of plasticity within this material, it can, therefore, be hypothesised that the iodide anion is immobile and thereby hindering plastic deformation of the material. This has been found to be the case in other solids, e.g., fast-ion conductors such as AgI, where the iodide anion is static, while

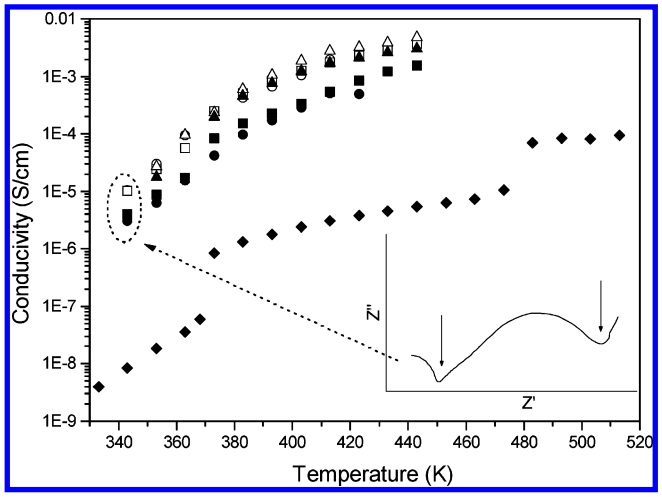

Figure 2. Conductivity plot of the pure $P_{1,1}I$ (◆), the $P_{1,1}I$ doped with 2 wt % LiI (▲, △), 5 wt % LiI (■, □), and 10 wt % LiI (●, ○). The inset shows the Nyquist plot for the 10 wt % LiI sample at 70 °C.

the Ag cations are the mobile species.[22] It can be hypothesised that the $P_{1,1}I$ salt behaves in a similar way, having highly mobile cations while the iodide anions are fixed on their lattice sites.

In Figure 2, the conductivity of the samples is shown as a function of temperature. It can be noted that there is a step in conductivity at each phase transition temperature for the pure matrix ($P_{1,1}I$). This has previously been observed in ionic plastic crystals when they enter their different plastic/rotator phases[23] and is probably due to a sudden increase of the ionic mobility in the higher temperature phase. The onset of different rotational motions of the cation is likely to create vacancies and dislocations in the lattice, thereby increasing also the translational mobility of the cations, resulting in the observed step in conductivity. An investigation on the related salt, ethyl methyl pyrrolidinium TFSA (P_{12}TFSA), has shown that the change in conductivity is also closely related to changes in vacancy size (free volume), as measured by positron annihilation lifetime spectroscopy (PALS).[24]

The addition of a small amount of LiI to the matrix increases the conductivity by almost 3 orders of magnitude. The Nyquist plots of the doped samples all show multiple touch-downs and depressed semicircles, indicating a more complex conduction mechanism. Two semicircular arcs could be easily resolved for all doped samples at all temperatures, (see inset in Figure 2) and the conductivity values corresponding to the touch downs for the two semicircles have been plotted in Figure 2, with open symbols for the higher-frequency semicircle and filled symbols for the lower-frequency semicircle. It is interesting to note that both conductivity values show similar temperature dependence, i.e., the activation energy is the same. It can be hypothesised that the two conductivity values are due to "bulk" and "grain boundary" conductivities or, alternatively, to the conductivity within two different phases. It is interesting to note also that the "higher" conductivity value is the same (within error) for all doped samples, while the "lower" conductivity decreases with increasing doping content. This latter observation lends support to the existence of an additional phase. As more LiI is added to $P_{1,1}I$, the amount of this phase will increase and, if it is less conductive, will lead to lower overall conductivity. The higher frequency intercept of the Nyquist plot, therefore, is possibly associated with the bulk $P_{1,1}I$-based (doped) phase. The presence of mixed lithium-containing phases has been previously suggested for related pyrrolidinium-based systems.[5,21] This will be further discussed within the context of lithium NMR below.

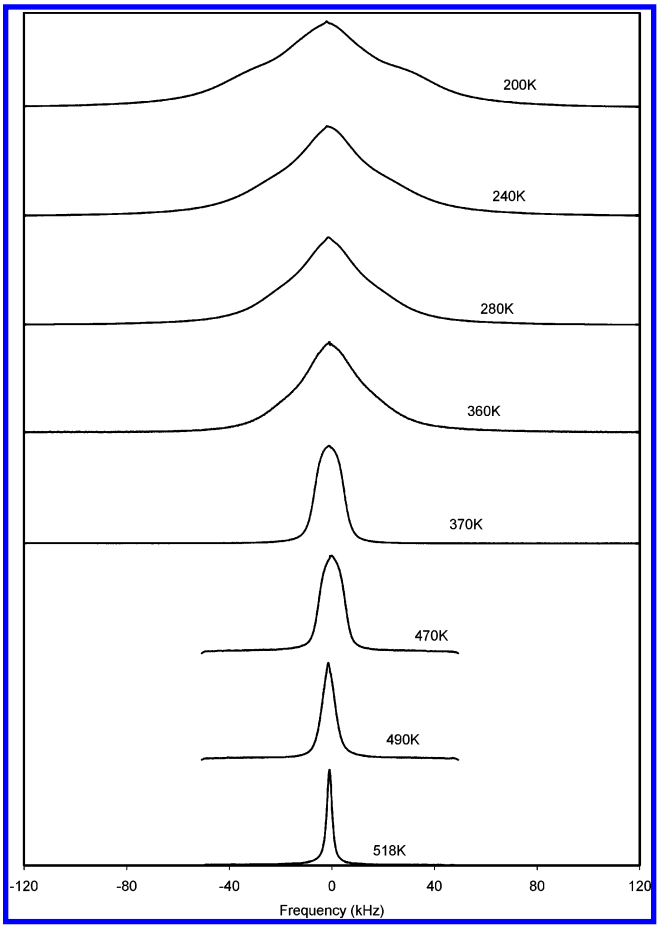

Figure 3. Representative single-pulse static ^{1}H NMR spectra for pure $P_{1,1}I$ for selected temperatures.

Figures 3 and 4 show selected one-pulse static ^{1}H NMR spectra for the pure $P_{1,1}I$ sample and $P_{1,1}I$ doped with 10 wt % LiI, respectively. The fwhm and percentage of total spectral area for the peaks in all ^{1}H spectra are presented in Figures5 and 6, respectively, allowing the changes in the relative areas and line widths of the peaks to be seen in more detail. It is immediately apparent from inspection of these spectra that, at lower temperatures, two dynamic states for the $P_{1,1}^+$ cation are found in the pure system and three dynamic states in the doped system. From Figure 5, it can be seen that the width of the broad and the narrow peaks in the doped sample correlates very well with the broad and the narrow peak in the pure sample. However, the doped sample has an extra feature, a second narrow (∼3 kHz), low-intensity (<2%) peak superimposed over the two larger peaks at low temperatures, increasing in intensity with temperature, as seen in Figure 6.

The relative area of the broad component of the ^{1}H NMR spectra drops slowly from a maximum >90% at 210 K to ∼80% above 300 K and then remains relatively constant until disappearing suddenly around 360 K, corresponding to the III → II transition. A sudden drop in line width has previously been reported for related materials upon entering their rotator phases.[25,26] At this temperature, a small decrease in the line width of the narrow component is also observed, from ∼16 to ∼11 kHz. Above 470 K, the line width of this component drops steadily, and reaches 2.4 kHz at 518 K in the pure sample. For the doped sample, however, the relative intensity of the second narrow component starts to grow steadily above 320 K, and above 490 K, it approaches 100% of the total area, i.e., the other narrow component disappears.

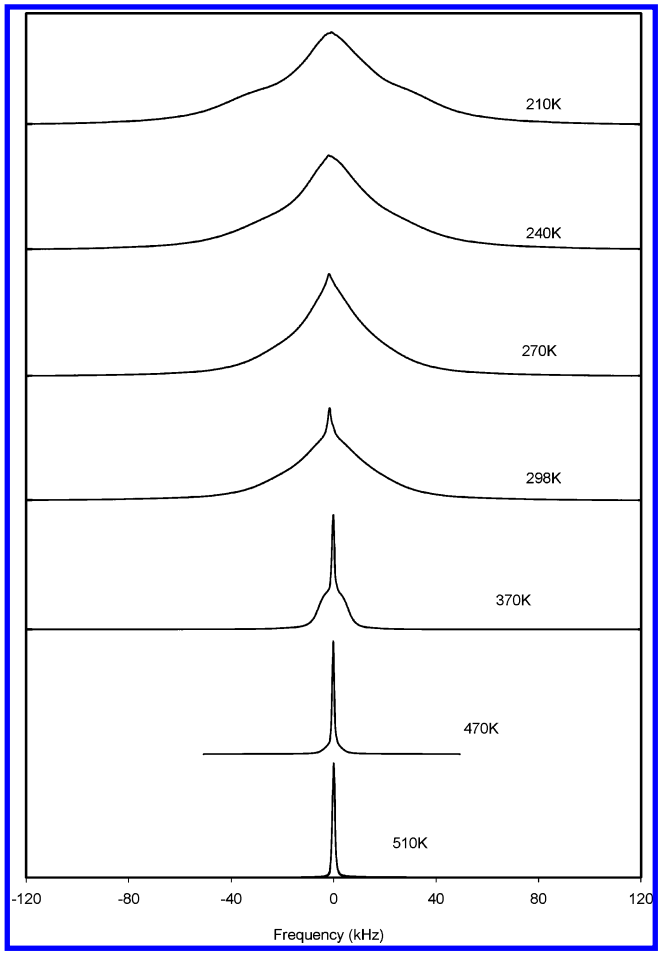

Figure 4. Representative single-pulse static ^{1}H NMR spectra for $P_{1,1}I$ doped with 10 wt % LiI for selected temperatures.

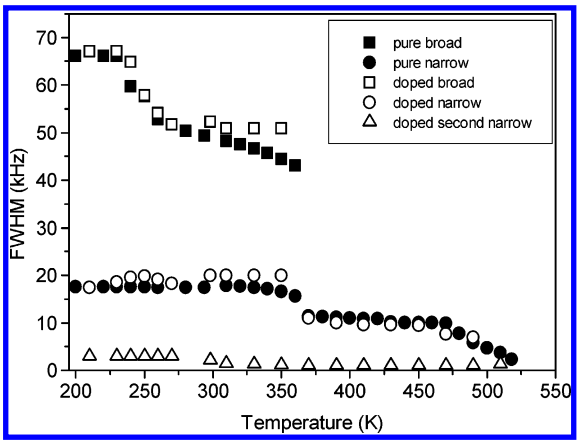

Figure 5. FWHM as measured for the broad (■, □), narrow (●, ○), and second narrow (Δ) peaks found in the static ^{1}H NMR spectra as a function of temperature for the $P_{1,1}I$ sample (filled symbols) and $P_{1,1}I$ doped with 10 wt % LiI (open symbols).

As mentioned above, an earlier study using second-moment calculations of the pure matrix material has been used to correlate the onset of different rotational motions to changes in the ^{1}H line width.[14] It was shown that changes observed for the broad component in the temperature range 230−290 K could be associated with a transition of the static $P_{1,1}^+$ cations to a state where the methyl groups on these cations are spinning. The narrow line, with a fwhm ∼17 kHz, was attributed to C_2 axis rotation of the cations, and a line width of 5 kHz corresponds to isotropic tumbling of the cations. Line widths less than 5 kHz were attributed to the translational diffusion of the cations because rotations alone could not narrow the resonance sufficiently. Therefore, given the line width of the second narrow component in the doped sample, this is assigned to diffusion of the $P_{1,1}^+$ cations. Direct evidence of diffusive cation motions in related organic iodides has been reported for the ethyl methyl imidazolium iodide system.[27−29]

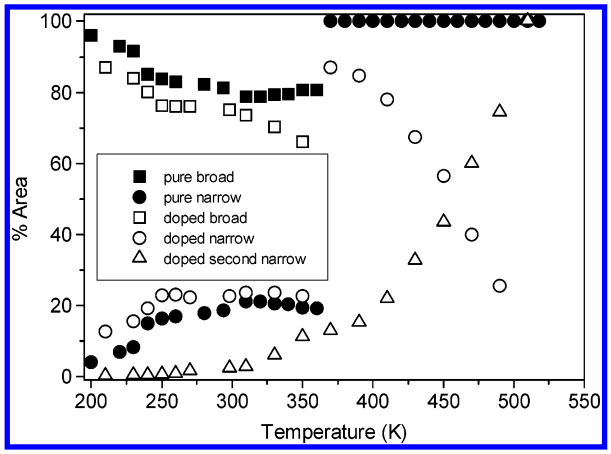

Figure 6. Relative percentage of the area of the broad (■, □), narrow (●, ○), and second narrow (△) peaks found in the static ^{1}H NMR spectra as a function of temperatures for the $P_{1,1}I$ sample (filled symbols) and $P_{1,1}I$ doped with 10 wt % LiI (open symbols).

Figure 6 shows the relative contributions from each peak to the total peak area as a function of temperature. The contribution from this second narrow peak is very low at low temperatures, but reaches ∼20% at the III → II transition, and at temperatures above the II → I, it is close to 100%. This indicates that a small fraction of the matrix cations ($P_{1,1}^+$) are diffusing already at very low temperatures in the doped samples and that there is a steadily growing amount of matrix cations that exhibit diffusional mobility. The broad and narrow peaks follow the same temperature trend as the pure matrix, as seen in Figure 5. Unfortunately, ^{125}I NMR spectra are not very informative with respect to iodide mobility because the line width is dominated by factors other than translational mobility. Therefore, while the proton NMR clearly evidences proton translation mobility, it is also possible that the iodide is also mobile in the plastic phases and contributes to the total conductivity.

From these results, it can be seen that the addition of a small amount of dopant has a significant effect on the matrix material; at low temperatures, in phase III, the effect is not very strong and only a small fraction of the matrix cations have an increased mobility. However, once phase II is entered, an increasing fraction of the matrix cations show mobility attributed to translational diffusion (interpreted as the narrow ^{1}H line width). This is quite the opposite of the pure matrix, where the ^{1}H line width corresponding to diffusional motion of the $P_{1,1}^+$ cation is reached only in phase I. As discussed above, this is suggested to be due to an increased number of vacancies created by the introduction of the dopant ions.

Figure 7 shows selected one-pulse static ^{7}Li NMR spectra for the $P_{1,1}I$ sample doped with 10 wt % LiI. Again the spectra are composed of several superimposed peaks of different width. In Figure 8, the fwhm and percentage of total spectral area for the narrow component of the peak is presented as a function of temperature. It can be seen that the width of the peak decreases with increasing temperature. It is quite broad at low temperatures (∼1 kHz), decreasing rapidly from low temperatures up to about 330 K, thereafter seemingly stabilizing until decreasing even further at 430 K. At higher temperatures, the line width is ∼300 Hz, indicating a rather mobile Li ion. It can also be seen from

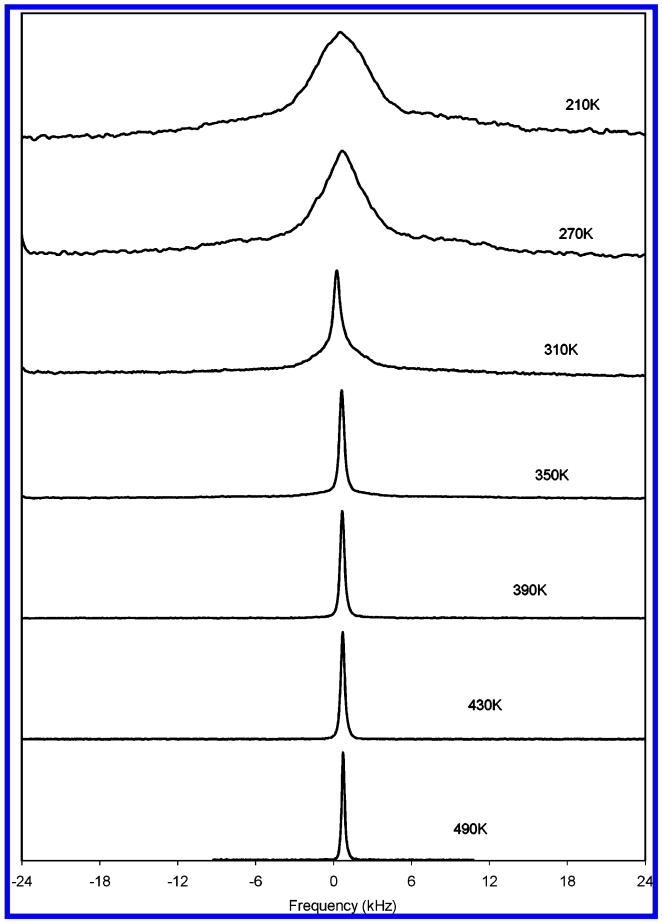

Figure 7. Representative single-pulse static ^{7}Li NMR spectra for $P_{1,1}I$ doped with 10 wt % LiI at selected temperatures.

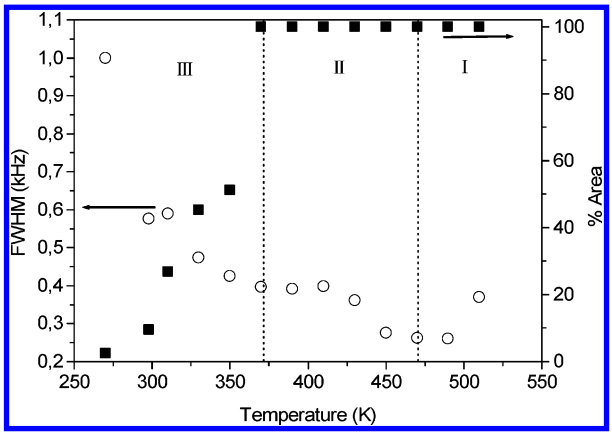

Figure 8. FWHM (○) and relative percentage of the area (■) for the narrow peak found in the static ^{7}Li NMR spectra as a function of temperature for the $P_{1,1}I$ 10 wt % LiI sample.

Figure 8 that, at the III → II transition, the relative area of the narrow lithium line has reached 100%, indicating that all Li ions now exhibit equal mobility.

The above results have shown that both the dopant ions (i.e., the lithium ions) and the matrix cations ($P_{1,1}^+$) are mobile in the doped samples. This can be discussed in terms of an increased number of vacancies and other defects introduced by the dopant, possibly due to the difference in size between the lithium ion and the matrix cation. The conductivity (Figure 2) shows two conduction mechanisms or processes for the doped samples with different concentration dependence. The higher value is independent of the dopant level, while the lower value decreases with increasing dopant concentration. There seems

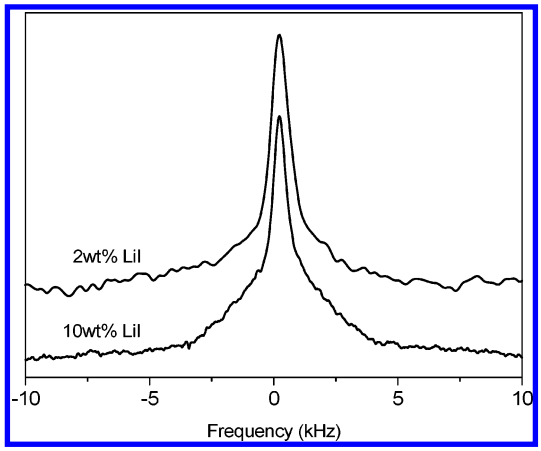

Figure 9. ^{7}Li NMR line width at room temperature (298 K) for the 2 and 10 wt % LiI-containing samples.

to be an optimal doping level beyond which the matrix material becomes saturated, and it is hypothesised that, above this level, a second phase is formed. To further investigate this, a static ^{7}Li NMR line width measurement of the 2 wt % sample was conducted at room temperature, and the spectrum is compared to the spectrum of the 10 wt % sample in Figure 9. It can be seen that both spectra are composed of a broad and a narrow line, where the spectrum of the 2 wt % sample has a larger percentage of the area in the narrow peak. The diffusion coefficient for Li^+ was calculated from this narrow line width component, assuming that $T_2^* = {}^1/_2\pi\nu$ and that we are in the high-temperature limit where $\omega\tau_c \ll 1$, such that

$$\frac{1}{T_2} = \gamma^2 H^2 \left(\tau_c + \frac{\tau_c}{1 + (\omega\tau)^2} \right) \tag{1}$$

can be simplified to

$$\frac{1}{T_2} = 2\gamma^2 H^2 \tau_c \tag{2}$$

from which the correlation time can be calculated. The diffusion coefficient can then be estimated using the following relation:

$$D = 6a^2/\tau_c \tag{3}$$

where a is the distance which the lithium ion moves during the correlation time τ_c and is assumed to be the same as the diameter of the pyrrolidinium cation, 6 Å. The values determined were on the order of 10^{-7} m^2 s^{-1} and were subsequently used to calculate a conductivity from the Nernst−Einstein equation

$$\sigma = \Sigma n_{Li} q_i D_i \tag{4}$$

where n_{Li} is obtained from the deconvolution and integration of the NMR peaks. This yielded a conductivity value of order 10^{-3} S cm^{-1}, which is significantly higher than the measured value (Figure 2). The likely reason for this overestimation is due to the assumptions leading to eq 1, which are only valid in the limit where $\omega\tau_c \ll 1$.

With Li being a quadrupolar nucleus, there are two possible explanations for the broad line; it might be due either to quadrupolar satellites (smeared over a wide frequency range rather than discrete, as would be found in the case of a perfect crystalline material) or due to less-mobile lithium ions. However, the quadrupolar coupling constant for crystalline systems is typically around 50−150 kHz, which is much broader than the line observed in these samples. Furthermore, there is no evidence

of quadrupolar peaks at elevated temperatures (Figure 7). Therefore, it is assumed that the broad component is due to less-mobile lithium ions. For the narrow component of the line, the line width (fwhm) is the same (within error) for both samples, indicating equal lithium mobility. This is consistent with the conductivity data and the hypothesis that there are two phases at higher dopant concentrations. The second phase has lower conductivity, and as more of this phase is produced with increasing dopant level, presumably at the grain boundary of the matrix dominated phase, this would lead to a decrease in conductivity as ionic motion is partially blocked. This has been found for similar plastic crystals when mixed with polymers, where SEM pictures showed that the polymeric material produces a grain boundary around the plastic crystals, hindering ionic transport between the crystallites.[13]

Summary

An almost 3 orders of magnitude increase in ionic conductivity has been observed with the addition of a small amount of LiI to *N*,*N*-dimethyl-pyrrolidinium iodide. A narrow lithium NMR line width indicates rather mobile lithium ions in this system. The ^{1}H NMR data, as well as the thermal analysis, suggests that the addition of a dopant also affects the matrix cations. It is suggested that the decrease of the transition temperatures for the two phase transitions with the addition of LiI is evidence of a solid solution of the LiI/$P_{1,1}$I mixture, at least at lower dopant levels. A fraction of the matrix cations has been found to exhibit an increased mobility, as observed by a third, very narrow ^{1}H NMR line superimposed on the broader ones. Furthermore, the enthalpy and entropy of the phase transitions decreases with the addition of dopant. This has been discussed in terms of an enhanced number of vacancies and defects due to the introduction of dopant ions. It is hypothesized that there is a maximum solid solubility of LiI in $P_{1,1}$I, and above this, there is a second, low-conducting phase produced with a high Li content. This phase is suggested to form within the grain boundaries, thereby hindering the intergrain ion transport.

Acknowledgment. We would like to thank the ARC for financial support.

References and Notes

(1) Keen, D. A. *J. Phys.: Condens. Matter*. **2002**, *14*, R819−R857.
(2) Angell, C. A. *Solid State Ionics* **1998**, *105*, 15−24.
(3) Shahi, K.; Wagner, J. B., Jr. *Appl. Phys. Lett.* **1980**, *37*, 757−759.
(4) MacFarlane, D. R.; Huang, J. H.; Forsyth, M. *Nature* **1999**, *402*, 792−794.
(5) Forsyth, M.; Huang, J.; MacFarlane, D. R. *J. Mater. Chem.* **2000**, *10*, 2259−2265.
(6) Abu-Lebdeh, Y.; Alarco, P. J.; Armand, M. *Angew. Chem., Int. Ed.* **2003**, *42*, 4490−4501.
(7) Abu-Lebdeh, Y.; Alarco, P. J.; Armand, M. *J. New Mater. Electrochem. Syst.* **2004**, *7*, 29−31.
(8) Huang, J. H.; Forsyth, M.; MacFarlane, D. R. *Solid State Ionics* **2000**, *136*, 447−452.
(9) MacFarlane, D. R.; Meakin, P.; Sun, J.; Amini, N.; Forsyth, M. *J. Phys. Chem. B* **1999**, *103*, 4164−4170.
(10) Golding, J.; Hamid, N.; MacFarlane, D. R.; Forsyth, M.; Forsyth, C.; Collins, C.; Huang, J. *Chem. Mater.* **2001**, *13*, 558−564.
(11) Forsyth, S.; Golding, J.; MacFarlane, D. R.; Forsyth, M. *Electrochim. Acta* **2001**, *46*, 1753−1757.
(12) Efthimiadis, J.; Pas, S. J.; Forsyth, M.; MacFarlane, D. R. *Solid State Ionics* **2002**, *154*, 279−284.
(13) (a) Efthimiadis, J.; Annat, G. J.; Forsyth, M.; MacFarlane, D. R. *Phys. Chem. Chem. Phys.* **2003**, *5*, 5558−5564. (b) Efthimiadis, J.; Forsyth, M.; MacFarlane, D. R. *J. Mater. Sci.* **2003**, *38*, 3293−3301
(14) Adebahr, J.; Seeber, A.; MacFarlane, D. R.; Forsyth, M. *J. Appl. Phys.* **2005**, *97*, 9.
(15) Kaber, R.; Nilsson, L.; Andersen, N. H.; Lunden, A.; Thomas, J. O. *J. Phys.: Condens. Matter* **1992**, *4*, 1925−1933.
(16) Wilmer, D.; Funke, K.; Witschas, M.; Banhatti, R. D.; Jansen, M.; Korus, G.; Fitter, J.; Lechner, R. E. *Physica B* **1999**, *266*, 60−68.
(17) Lee, J.-S.; Adams, S.; Maier, J. *J. Phys. Chem. Solids* **2000**, *61*, 1607−1622.
(18) Maier, J. *Solid State Ionics* **2004**, *175*, 7−12.
(19) Porter, D. A., Easterling, K. E. *Phase Transformations in Metals and Alloys*, 2nd ed.; Chapman Hall: London, 1992; p 368.
(20) Ricci, E. J. In *Molten Salt Chemistry*; Blander, M., Ed.; John Wiley & Sons: New York, 1964.
(21) Henderson, W. A.; Passerini, S. *Chem. Mater.* **2004**, *16*, 2881−2885.
(22) Ivanov-Schitz, A. K.; Mazniker, B. J.; Povolotskaya, E. S. *Solid State Ionics* **2003**, *159*, 63−69.
(23) MacFarlane, D. R.; Forsyth, M. *Adv. Mater.* **2001**, *13*, 957−966.
(24) Hill, A. J.; Huang, J.; Efthimiadis, J.; Meakin, P.; Forsyth, M.; MacFarlane, D. R. *Solid State Ionics* **2002**, *154*, 119−124.
(25) Shimizu, T.; Tanaka, S.; Onoda-Yamamuro, N.; Ishimaru, S.; Ikeda, R. *J. Chem. Soc., Faraday Trans.* **1997**, *93*, 321−326.
(26) Hattori, M.; Fukada, S.; Nakamura, D.; Ikeda, R. *J. Chem. Soc., Faraday Trans.* **1990**, *86*, 3777−3783.
(27) Every, H. A.; Bishop, A. G.; MacFarlane, D. R.; Oraedd G.; Forsyth, M. *J. Mater. Chem.* **2001**, *11*, 3031−3036.
(28) Grune, M.; Muller-Warmuth, W.; Zumhebel, P.; Krebs, B. *Solid State Ionics* **1993**, *66*, 165−173.
(29) Forsyth, M.; Wong, S.; Nairn, K. M.; Best, A. S.; Newman, P. J.; MacFarlane, D. R. *Solid State Ionics* **1999**, *124*, 213−219.